ELSEVIER

Computerized Medical Imaging and Graphics 29 (2005) 259–266

Computerized Medical Imaging and Graphics

www.elsevier.com/locate/compmedimag

Evaluation of osteoporosis in X-ray CT examination: A preliminary study for an automatic recognition algorithm for the central part of a vertebral body using abdominal X-ray CT images

Sadamitsu Nishihara[a,*], Hiroshi Fujita[b], Tadayuki Iida[a,1], Atsushi Takigawa[a], Takeshi Hara[b], Xiangrong Zhou[b]

[a]*Department of Radiological Sciences, Hiroshima Prefectural College of Health Sciences, 1-1 Gakuen-machi, Mihara-City, Hiroshima 723-0053, Japan*
[b]*Division of Regeneration and Advanced Medical Sciences, Department of Intelligent Image Information, Graduate School of Medicine, Gifu University, 1-1 Yanagido, Gifu-City, Gifu 501-1194, Japan*

Received 9 November 2004; accepted 27 December 2004

Abstract

We have developed an algorithm that can distinguish the central part of the vertebral body from abdominal X-ray CT images to determine whether it is possible to aid a diagnosis of osteoporosis. We classified three measures for the principal component analysis and linear discriminant function. When we judged whether patients had osteoporosis or not, the ratio usable for diagnosing osteoporosis (sensitivity) was 1.00 (15/15), and for diagnosing as normal (specificity) was 0.64 (7/11). We believe that this algorithm can be used to aid in diagnosing osteoporosis, utilizing the measures obtained from the CT images.

Keywords: X-ray CT images; Automatic recognition; Image processing; Computer-aided diagnosis; Osteoporosis

1. Introduction

Recently, we are able to obtain detailed information on a broad area in a short period of time by using a helical (or spiral) CT and multidetector-row CT [1]. In general, physicians need information about the main targets of requested X-ray CT examinations. The main targets include the lung area and mediastinum for chest CT examination, and the liver or spleen for abdominal CT examination, in most cases. However, we do not make good use of information from other targets (for example, the vertebral column) from a single X-ray CT examination. In other words, there is a possibility that a portion of the information contained in the image is not being used effectively. For patients, it is vital that more information be elicited from a single examination.

The aim of our study was to obtain more useful information about other portions of the image which are not the main targets in common X-ray CT examinations. Concretely, we have shown that we can aid in diagnosing osteoporosis by utilizing the measures obtained from abdominal CT images [2]. Doi describes the basic concept of computer-aided diagnosis (CAD) as follows. CAD may be defined as a diagnosis made by a radiologist who takes into account the results of the computer output as a 'second opinion', and the basic concept of CAD is clearly different from that of 'automated diagnosis,' which had been investigated in the 1960s and 1970s [3]. Our concept is to aid physicians in making a diagnosis by using computer output, and, consequently, our study is a part of CAD. Guglielmi et al. [4] investigated the diagnostic sensitivity of posteroanterior dual energy X-ray absorptiometry (PA-DXA), lateral-DXA, and quantitative computed tomography (QCT). Andresen et al. [5] proposed a risk score that separately assessed bone mineral density (BMD) and structural parameters for spongious and cortical bone, and aggregated them into a single diagnostic parameter.

* Corresponding author. Tel.: +81 848 60 1205; fax: +81 848 60 1134.
E-mail address: nisihara@hpc.ac.jp (S. Nishihara).
[1] Present address: Department of Public Health, Fujita Health University School of Medicine, 1-98 Dengakugakubo, Kutsukake-cho, Toyoake-City, Aichi 470-1192, Japan.

0895-6111/$ - see front matter © 2005 Elsevier Ltd. All rights reserved.
doi:10.1016/j.compmedimag.2004.12.001

The concepts of these studies are to diagnose osteoporosis or fracture risks with the QCT and/or DXA, but these concepts are different from ours. Other studies have been conducted to show that a diagnosis of osteoporosis could be made by using a chest X-ray CT image done for other diagnostic screening [6,7]. The concepts of these papers and of our study are similar, but we believe that the reliability of these papers are different from of ours. Nakayama et al. [6] investigated the CT number of the central part of the thoracic vertebral bodies to support a diagnosis of osteoporosis. However, it was not clear whether the CT number reflected the level of osteoporosis, because the researchers did not check the relationship between the CT number and BMD of the same patient. Shiomi et al. [7] discussed an automatic algorithm to extract the values of the central part of the thoracic vertebral bodies and compared the CT number and BMD. However, the positions of the extracted CT numbers and of the examined BMD were from different parts (CT: thoracic vertebral body; BMD: calcaneus). In our study, however, we compared the CT number and BMD of the same part (lumbar vertebral body). Therefore, we believe that the accuracy of our study is higher than that of those reported above.

Osteoporosis is associated with a low BMD. Several methods, including PA-DXA and QCT, have been considered for the noninvasive measurement of BMD [4,8,9]. In Japan, we generally judge whether a patient has osteoporosis by using the PA-DXA type BMD measurement equipment [10].

In this study, we developed an algorithm that can distinguish the central part of the vertebral body from the abdominal CT image and calculate some measures automatically. For this purpose, we examined 62 cases, without distinction of sex. In addition, we report the correlation between the BMD and several measures that were calculated, and examine whether it is possible to aid physicians in making a diagnosis of osteoporosis with the CT images. Twenty-six female patients participated. Furthermore, we discuss the potentiality of the screening examination using the common abdominal X-ray CT examination for diagnosing osteoporosis.

2. Experimental methods

2.1. Diagnostic criteria for primary osteoporosis: year 2000 revision

The diagnostic criteria for primary osteoporosis were proposed by the Japanese Society for Bone and Mineral Research in 2000 (Table 1). The patients were classified into three groups according to the diagnostic criteria based on the BMD found in the lumbar spine with a PA-DXA examination. The purposes of our study were to distinguish the central part of the vertebral body from an abdominal routine CT examination, and to predict whether a patient was osteoporotic or not with the measures obtained from these CT images. Therefore, all patients were classified independent of the presence of a fragility fracture in this study [10].

Table 1
Diagnostic criteria for primary osteoporosis (Year 2000 revision) [10]

I. With fragility fracture[a]	
II. Without fragility fracture	Bone mineral density (BMD)[b]
Normal	80% of YAM[c] or higher
Decreased bone mass (Osteopenia)	70–80% of YAM
Osteoporosis	Less than 70% of YAM

[a] A fragility fracture is a nontraumatic bone fracture that is caused by a slight external force to a bone with low BMD (BMD less than 80% of YAM).
[b] Bone mineral density usually refers to lumbar BMD. However, when the measurement is inappropriate because of such reasons as spinal deformity, the femoral neck BMD should be used. When measurement at that site is difficult, BMD of the radius, second metacarpal bone, or calcaneus should be used.
[c] YAM, Young adult mean (aged 20–44 years).

The World Health Organization (WHO) published the diagnosic criteria for osteoporosis based on the BMD measurement in 1994. The following points are cited as the criteria [11].

1. Peak bone mass (PBM) depends on the population that is regarded as the standard.
2. There is a possibility that the value of the PBM changes when there is a difference in the densitometer and in the method of BMD measurement.
3. The diagnosis of low bone mass may vary with a difference in the part measured.

Consequently, the diagnostic criteria proposed by the Japanese Society for Bone and Mineral Research in 2000 were made in full and strict consideration of these points. Therefore, we believe that these criteria were suitable to be applied to our study.

2.2. Materials and methods

We examined 62 cases (males: 30, females: 32), ranging in age from 35 to 86 years (average age: 62.8 years). The volume that contained the third lumbar vertebra was examined by using a spiral CT scanner (CT-W950SR: Hitachi Medical Corporation, Tokyo). Tube voltage was 120 kV. The field of view (FOV) and matrix size were 250 mm and 512×512 pixels, respectively. Slice thickness was 5 mm, and the movement distance of the table was 5 mm/rotation, which was recalculated to make the reconstruction interval a minimum unit (1 mm). We made about 50 images of the transverse sections. The largest island images were selected by the threshold processing of each original image. To evaluate whether the CT image included the lumbar vertebral body or not, measures of the area and degree of circularity were used to make the determination in each image. A region of interest (ROI) was

set up automatically in the recognized images. The mean CT number, coefficient of variation, and first moment of the power spectrum were calculated as measures representing specific features of osteoporosis disease in the ROI of the recognized spongious bone.

We also judged whether a female patient had osteoporosis or not by using the diagnostic criteria (only female data available). There were 26 female patients who participated as subjects, with an age range of 35–79 years (average age: 61.3 years). Some patients had more than one CT examination, resulting in a total of 32 X-ray CT examinations. Four of the patients had two examinations, and one of the patients had three. BMD measurements with PA-DXA and with L-DXA were made with a model QDR-4500 densitometer (Hologic, Inc., Massachusetts) for the same patients. Figs. 1 and 2 show a schematic diagram. The contents of the figures are explained clearly in the following paragraphs.

2.2.1. Extraction of the central part of the vertebral body

The island images were selected by the threshold processing of each original image. The areas of each island were calculated, and the island that had the largest area was selected as the subject region. The perimeter of the largest island image was measured, and the degree of circularity was calculated by using the following equation (Fig. 1)

$$\text{Degree of circularity} = 4\pi \frac{\text{Area of vertebra}}{(\text{Perimeter of vertebra})^2} \quad (1)$$

2.2.2. Setting of the ROI and feature analysis in the spongious bone (Fig. 2).

An ROI (32×32 pixels) was set up automatically in the recognized images. When the ROI was set in the image of a spongious bone, the point where the width of the anterior side of the vertebral body was longer than the ROI was identified. After our algorithm had automatically judged whether a nutrient foramen was present or not, a suitable point for the posterior side of the vertebral body was located. The vertical center point of the ROI was chosen as the middle of these two points of the vertebral body. The horizontal center point of the ROI was chosen as the middle point between the lateral sides of the vertebral body.

We calculated the mean CT number, coefficient of variation, and first moment of the power spectrum in the recognized vertebral body. The first moment of the power spectrum M was calculated by the following equation

$$M = \frac{\int_{-\infty}^{\infty}\int_{-\infty}^{\infty}\sqrt{u^2+v^2}T^2(u,v)\mathrm{d}u\mathrm{d}v}{\int_{-\infty}^{\infty}\int_{-\infty}^{\infty}T^2(u,v)\mathrm{d}u\mathrm{d}v} \quad (2)$$

where $T(u,v)$ is the Fourier transform of the data in the ROI, and this first moment of the power spectrum shows

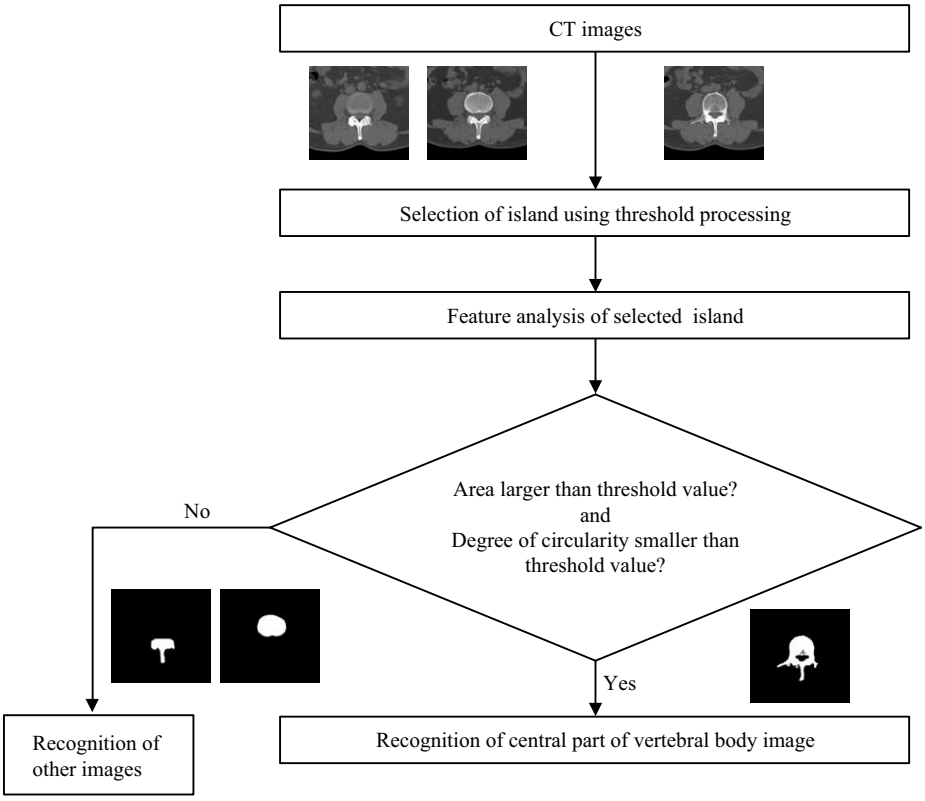

Fig. 1. Schematic diagram of the extraction of the central part of the vertebral body.

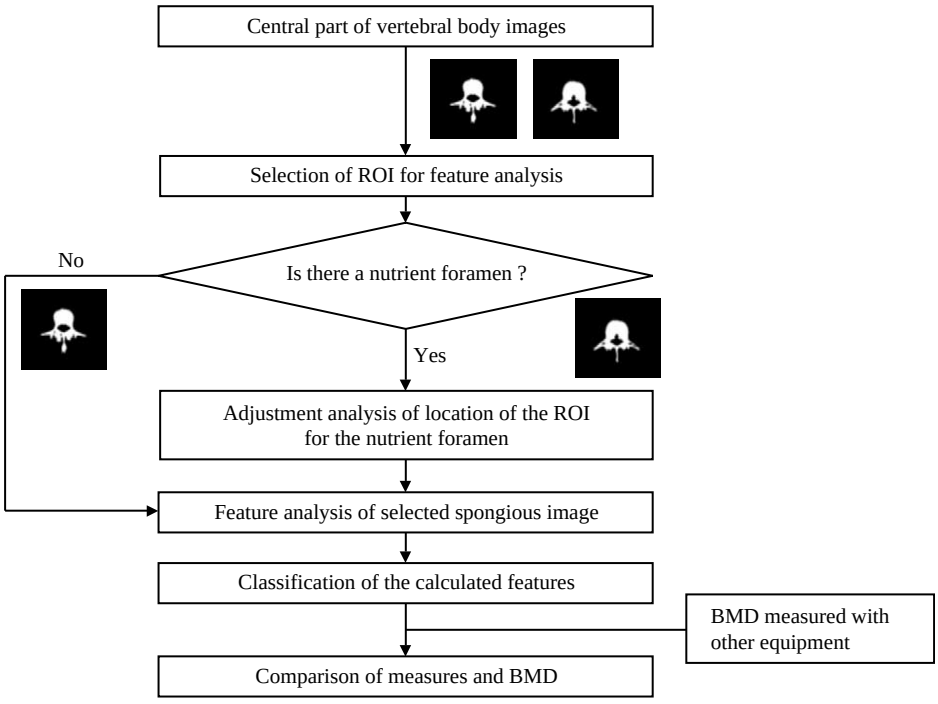

Fig. 2. Schematic diagram of the setting of ROI and feature analysis in spongious bone.

the mean value of the spatial frequency of the image's structure [12].

We classified three measures obtained from the CT images for normal and abnormal groups with the principal component analysis, and the results obtained from the diagnosis criteria for the two groups were compared.

3. Results

Our algorithm was able to distinguish the central part of the vertebral body in all 62 cases and to set up the ROI automatically. Fig. 3 showed examples of the automatically located ROI. A case that had no nutrient foramen is shown in Fig. 3(a), and a case that included the nutrient foramen is illustrated in Fig. 3(b). Both ROIs were set up without the influence of the presence of the nutrient foramen.

The variations of the BMD obtained from PA-DXA were 0.49–1.18 g/cm^2 and of L-DXA, 0.29–0.87 g/cm^2. Therefore, 11 patients were classified as normal, 5 patients were rated as osteopenic, and 10 patients were recognized as osteoporotic, using the diagnostic criteria. The mean CT numbers were 3.32–206.52 HU (average $\pm$ standard deviation: 117.68 $\pm$ 48.34 HU); the coefficients of variation were 0.19–12.98 (0.91 $\pm$ 2.47); and the first moments of the power spectrum were 0.21–0.38 cycle/mm (0.28 $\pm$ 0.05 cycle/mm) in the ROI of 26 female patients. Fig. 4 illustrates the relationship between the three measures (mean CT number, coefficient of variation, and first moment of the power spectrum) and the BMDs obtained from

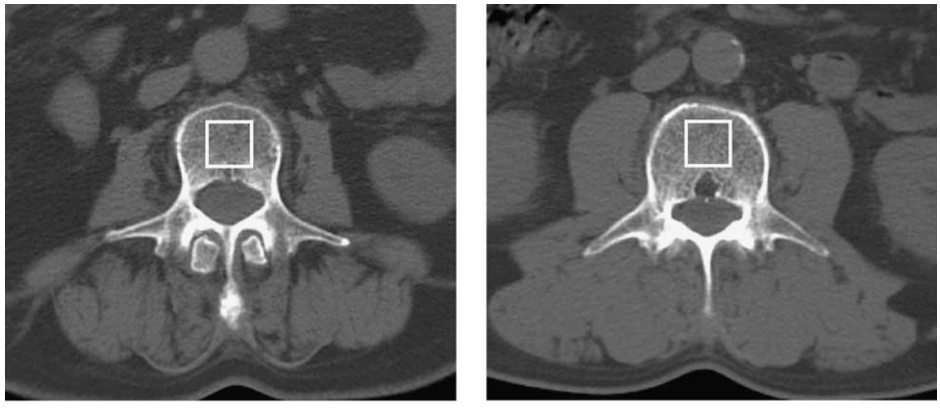

(a) (b)

Fig. 3. Examples of automatically located ROI.

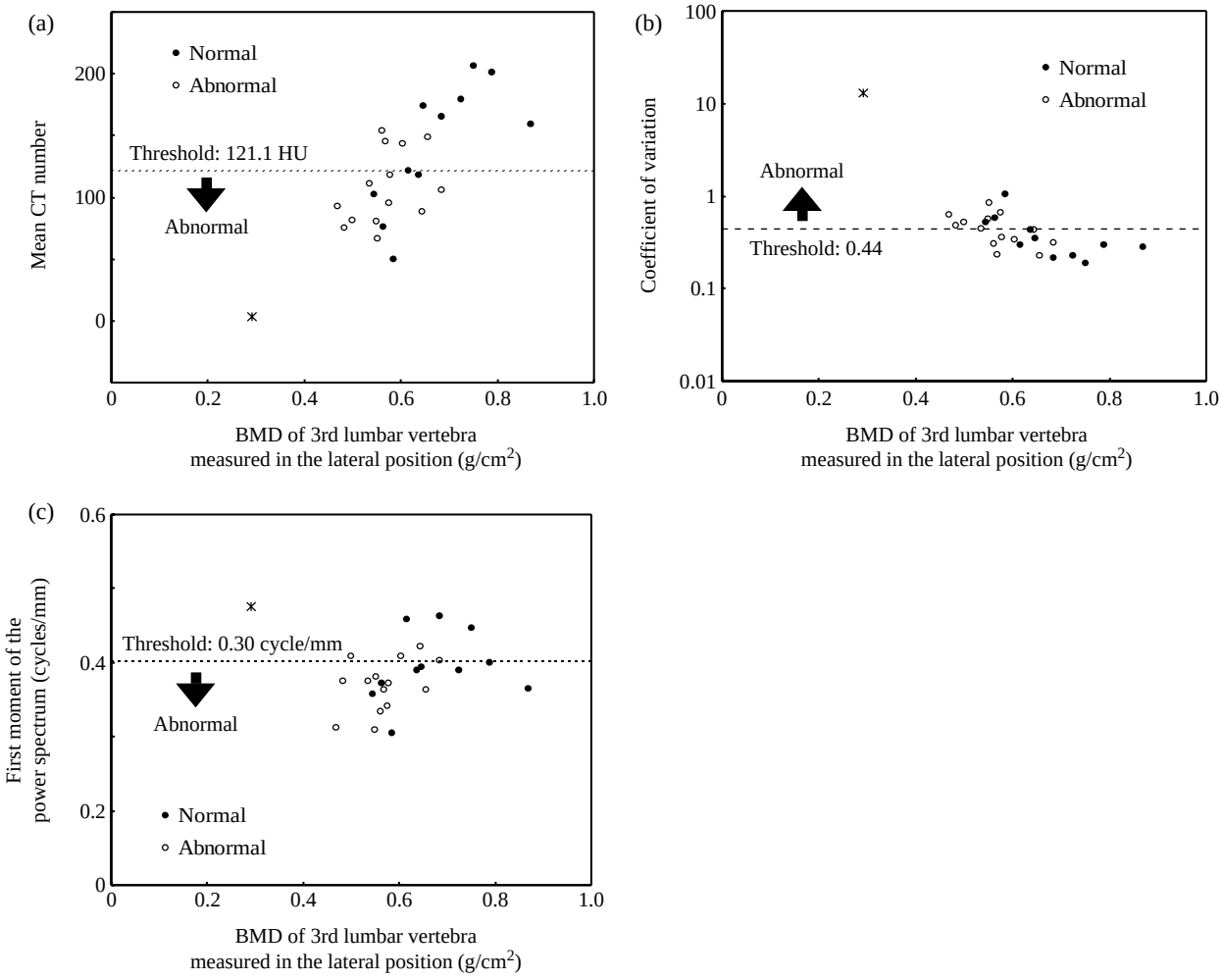

Fig. 4. Relationship between the three measures and BMDs: (a) mean CT number, (b) coefficient of variation (coefficient of variation = standard deviation/mean CT number), and (c) first moment of the power spectrum.

L-DXA. Fig. 5 shows the results of the analysis of the three measures obtained from the CT images, in which we used the principal component analysis. In Fig. 5, the horizontal and vertical components were calculated by the following equations:

$$y_1 = 0.791\mathrm{CT}_{\mathrm{num}} - 0.612\mathrm{CV} + 0.124\mathrm{FMPS} \quad (3)$$

$$y_2 = 0.297\mathrm{CT}_{\mathrm{num}} + 0.355\mathrm{CV} + 0.896\mathrm{FMPS} \quad (4)$$

where y_1 is the first principal component (horizontal axis), y_2 is the second principal component (vertical axis), $\mathrm{CT}_{\mathrm{num}}$ is the mean CT number, CV is the coefficient of variation, and FMPS is the first moments of the power spectrum. The proportion of the variance reflected by the two principal components was 91.0%. For the first principal component, the eigenvectors of the mean CT number and the coefficient of variation were 0.791 and −0.612, respectively. In other words, both eigenvectors of the mean CT number and the coefficient of variation had more influence than that of the first moment of the power spectrum. Meanwhile, the first moment of the power spectrum had the most effect on the second principal component (eigenvector: 0.896). The open points in Fig. 5 indicate the abnormal cases (osteopenia and osteoporosis), and the solid points show

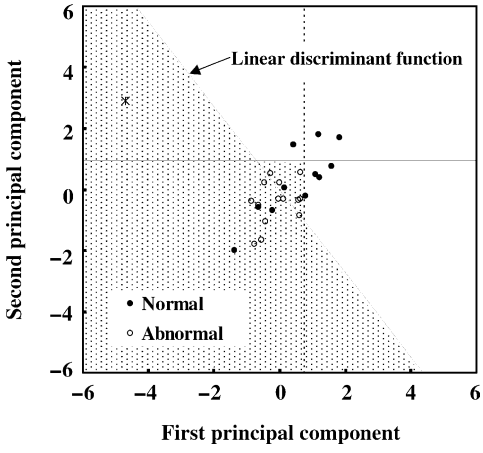

Fig. 5. Results of the principal component analysis.

the normal cases. The threshold values of the two principal components were judged from Fig. 5 (horizontal axis: 0.72, vertical axis: 0.97). We adopted a linear discriminant function for the two components to improve the accuracy. The result of the discriminant function is shown in the following equation

$$1.37 \times 10^{-6} = 3.55y_1 + 2.45y_2 \quad (5)$$

where y_1 is the first principal component (horizontal axis) and y_2 is the second principal component (vertical axis). As a result, the cases that were indicated in the dot region of Fig. 5 were recognized as abnormal. When we applied these threshold values and the result of the linear discriminant function to all of the female patients, the ratio (sensitivity) usable for diagnosing a patient as osteoporotic was 1.00 (15/15), and the ratio (specificity) usable for diagnosing a patient as normal was 0.64 (7/11).

4. Discussion

The degree of circularity and the island area were adopted as the features to pinpoint the central part of the vertebral body in this study (Fig. 1) [2]. For this reason, we were able to determine the quantity of anatomical information on the vertebral column. As a result, it was possible to distinguish the central part of the vertebral body in all 62 cases with two simple features. There are other methods available to extract the vertebral body. For example, histograms that correspond to the parts of the vertebral column in each axial chest X-ray CT image can be adopted to detect the space between the thoracic vertebral bodies [7]. This method is based on the fact that the space between the vertebral bodies is parallel to the axial image. However, there is some possibility that the space between the vertebral bodies is not parallel to the axial image for the lumbar vertebra. Although our 62 subjects included cases in which the space was not parallel to the axial image, our algorithm is still capable of extracting significant vertebral body values. Therefore, we believe that our method is effective in the quantitative extraction of the vertebral column.

The voxel size of the CT image which we used is about $0.5 \times 0.5 \times 5$ mm, and the data for the vertical structure of trabeculae has a lower accuracy than for the horizontal structure of trabeculae. Therefore, we only discussed the horizontal structure pattern at this stage. If the isotropic data could have been used for our study, we would have discussed the vertical structure pattern, as well.

Fig. 3(a) and (b) shows examples of automatically located ROI. The metabolic rate of spongious bone is six to eight-fold higher than that of cortical bone [5]. When a QCT examination is done, the ROI should be set up in the area of spongious bone, but cortical bone and the nutrient foramen should not be included [13]. Accordingly, we made fine, automatic adjustments to the position of the ROI through this basic concept (Fig. 2). We also propose that this clinical concept be included when algorithms are developed.

We classified three measures for normal and abnormal groups with the principal component analysis. As a result, 14 (sensitivity: 0.93) of the 15 patients were diagnosed correctly as osteoporotic, and seven (specificity: 0.64) of 11 patients were recognized correctly as normal cases. To improve the accuracy of diagnosis, more examinations need to be conducted. When we applied the two threshold values to both axes, one patient (symbol * in Fig. 5) showed that our algorithm failed in the estimation of osteoporosis. The reason, we think, is that she was classified as an abnormal case in the horizontal component, but not recognized in the vertical component. The horizontal component was regarded as the height and variability of the CT number, and the vertical component was regarded as the roughness of the spongious structure. Thus, this case was evaluated as having an abnormal quantity of mineral content, but the quality of the spongious bone was normal. This patient had the lowest mean CT number (3.32 HU) and the highest coefficient of variation (12.98). Fig. 4(a) and (b) indicated that these data were clearly abnormal (symbol *). However, the first moment of the power spectrum showed this to be a normal case (Fig. 4(c)). When we used the result of the discriminant function and the thresholds that were obtained from the principal component analysis, the patient indicate with the asterisk (*) was also diagnosed correctly as abnormal.

In this study, the specificity was 0.64 (7/11). Four of the original normal patients that our algorithm classified as abnormal cases obtained a BMD value of 80.2% on L-DXA, while the seven other normal patients obtained a value of 100%. On the other hand, the mean BMD of the original 15 abnormal patients was 75.7% in comparison with the seven normal patients evaluated as 100% on the L-DXA. There is a possibility that these four patients were actually abnormal cases. Disease that is close to borderline should be detected when a screening examination is done.

After the threshold values that were obtained from the discriminant analysis were adopted for the three features, we calculated the sensitivities and specificities for each feature. Table 2 illustrates these results and the results of the principal component analysis. The sensitivity and specificity for the mean CT number were 0.73 and 0.55, respectively. For the coefficient of variation, the sensitivity was 0.53, and the specificity, 0.73. The results of the first moment of the power spectrum were 0.67 (sensitivity) and 0.27 (specificity). However, when we applied the linear discriminant function and the principal component analysis, the sensitivity was 1.00 and the specificity was 0.64. This means that the sensitivity improves by combining three features with the discriminant function and the principal component analysis. We think it is necessary that the next task be to improve the specificity.

Table 2
Comparison between the result of the principal component analysis and the results obtained from the discriminant analysis

	Sensitivity	Specificity
PCA[a] (PCA[a]+LDF[b])	0.93 (1.00)	0.64 (0.64)
Mean CT number	0.73	0.55
Coefficient of variation	0.53	0.73
First moment of the power spectrum	0.67	0.27

[a] PCA: principal component analysis.
[b] LDF: linear discriminant function.

Our first purpose was to develop an algorithm to extract the central part of the vertebral body from an abdominal X-ray CT image. Therefore, we concentrated on only one lumbar vertebra to distinguish the central part of the vertebral body. The lumbar vertebra that we decided to focus on was the third lumbar vertebra. We believe that our algorithm can also be used to analyze the second and/or fourth lumbar vertebrae when it becomes possible to estimate osteoporosis in the third lumbar vertebra more accurately.

Some researchers have discussed the incidental extracolonic findings in CT colonography [14,15]. In other words, incidental (extracolonic) findings mean that the disease which was incidentally found in parts other than the colon was not the main target for the CT colonography. A high clinical importance was reported for 10–11% of the patients examined using the CT colonography, without substantially increasing the cost per patient [14,15]. Our concept is almost the same as the concept for the utilization of the incidental findings in CT colonography, in which more useful information should be elicited from one examination. The concept of our study was to obtain more useful information about parts that are not the main targets of abdominal X-ray CT examinations. Therefore, we believe that our study is very important. However, there is some anxiety about the possibility that an abdominal CT examination using a low-dose technique may not be sufficient for the detection of incidental findings [15]. The CT images used in our study were obtained from conventional CT examinations. Therefore, we believe that there is not necessarily a limitation in the detection capability with CT examinations using a low-dose technique. However, we would like to improve the accuracy of our algorithm in diagnosing osteoporosis, because when a case is suspicious, an unnecessary additional examination may be required (specificity: 0.64).

5. Summary

In this study, we have developed an algorithm that can distinguish the central part of the vertebral body in an abdominal X-ray CT image and calculate some measures automatically. Our algorithm was capable of distinguishing the central part of the vertebral body in all 62 cases. In addition, we examined whether it is possible to aid physicians in making a diagnosis of osteoporosis using the CT images. As a result, 15 (sensitivity: 1.00) of the 15 patients were diagnosed correctly as osteoporotic, and 7 patients (specificity: 0.64) out of 11 were recognized correctly as normal cases. Therefore, we believe that we may be able to obtain more effective information about other parts that are not the main targets in common body CT examinations by using our algorithm.

Acknowledgements

The authors are grateful to Michele E. Shimizu for editing the manuscript. This study was supported in part by the Grant-in-Aid for Scientific Research from the Ministry of Education, Culture, Sports, Science and Technology of Japan and the Grant-in-Aid for Cancer Research from the Ministry of Health, Labour and Welfare of Japan.

References

[1] Hu H. Multi-slice helical CT: scan and reconstruction. Med Phys 1999;26(1):5–18.
[2] Nishihara S, Fujita H, Iida T, Takigawa A, Hara T. Computer-aided diagnosis of osteoporosis using abdominal X-ray CT images: preliminary study of automated region extraction and of comparison between BMD values and CT features. Trans Jpn Soc Med Biol Eng 2004;42(1):7–15.
[3] Doi K. Computer-aided diagnosis and its potential impact on diagnostic radiology. In: Doi K, MacMahon H, Giger ML, Hoffmann KR, editors. Computer-aided diagnosis in medical imaging. Proceedings of the first international workshop on computer-aided diagnosis. Amsterdam: Elsevier; 1999. p. 11–20.
[4] Guglielmi G, Grimston SK, Fischer KC, Pacifici R. Osteoporosis: diagnosis with lateral and posteroanterior dual X-ray absorptiometry compared with quantitative CT. Radiology 1994; 192:845–50.
[5] Andresen R, Haidekker MA, Radmer S, Banzer D. CT determination of bone mineral density and structural investigations on the axial skeleton for estimating the osteoporosis-related fracture risk by means of a risk score. Br J Radiol 1999;72(858):569–78.
[6] Nakayama S, Kubo M, Kawata Y, Niki N, Machida S, Sasagawa M. Construction of the diagnostic support system of osteoporosis using the multi-slice CT images. Proceedings (CD-ROM version) of JAMIT (The Japanese Society of Medical Imaging Technology); 2002.
[7] Shiomi N, Saita S, Yamada N, Kubo M, Kawata Y, Niki N, et al. A computer aided diagnosis for osteoporosis using low-dose multi-slice CT images. Technical report of IEICE (The Institute of Electronics, Information and Communication Engineers) 2003;133(98):31–6.
[8] Cann CE, Genant HK. Precise measurement of vertebral mineral content using computed tomography. J Comput Assist Tomogr 1980; 4(4):493–500.
[9] Genant HK, Block JB, Steiger P, Glueer CC, Ettinger B, Harris ST. Appropriate use of bone densitometry. Radiology 1989;170:817–22.

[10] Orimo H, Hayashi Y, Fukunaga M, Sone T, Fujiwara S, Shiraki M, et al. Diagnostic criteria for primary osteoporosis: Year 2000 revision. J Bone Miner Metab 2001;19:331–7.
[11] Miller PD, Harper KD. The World Health Organization Criteria for the diagnosis of osteoporosis should be endorsed. Osteoporosis, Area Review (PRO/CON: Discussion) 1996;2–5.
[12] Katsuragawa S, Doi K, MacMahon H. Image feature analysis and computer-aided diagnosis in digital radiography: detection and characterization of interstitial lung disease in chest radiographs. Med Phys 1988;15(3):311–9.
[13] Ito M. Quantitative computed tomography (QCT), peripheral QCT (pQCT). Jpn J Radio Technol 1997;53(4):485–9.
[14] Hara AK, Johnson CD, MacCarty RL, Welth TJ. Incidental extracolonic findings at CT colonography. Radiology 2000;215(2): 353–7.
[15] Gluecker TM, Johnson CD, Wilson LA, MacCarty RL, Welth TJ, Vanness DJ, et al. Extracolonic findings at CT colonography: evaluation of prevalence and cost in a screening population. Gastroenterology 2003;124(4):911–6.

Sadamitsu Nishihara received his BS degree from the National Institution for Academic Degrees and University Evaluation, Japan, in 1996. From September to December in 1999, he was an international visitor at the Kurt Rossmann Laboratories for Radiologic Image Research, the University of Chicago. Since April 2000, he has been an instructor at the Department of Radiological Sciences, Hiroshima Prefectural College of Health Sciences, Hiroshima, Japan. His research interests include image analysis and processing, and image evaluation in medicine. He is a member of the Japanese Society of Radiological Technology, Japanese Society of Medical Imaging and Information Sciences, Japanese Society for Medical and Biological Engineering, and Japanese Society of Medical Imaging Technology.

Hiroshi Fujita received the BS and MS degrees in electrical engineering from Gifu University, Japan, in 1976 and 1978, respectively, and PhD degree from Nagoya University in 1983. He was a Research Associate at the University of Chicago, USA, from 1983 to 1986. He is currently Chairman and Professor in the Department of Intelligent Image Information, Graduate School of Medicine, Gifu University, Japan. His research interests include computer-aided diagnosis system, image analysis and processing, and image evaluation in medicine.

Tadayuki Iida received his BS degree from Fujita Health University School of Health Sciences, Faculty of Radiological Technology, Japan, in 1993, and received his PhD degree from Fujita Health University, Japan, in 2004. Since July 2004, he has been an instructor at the Department of Public Health, Fujita Health University School of Medicine, Aichi, Japan. His research interests include health science. He is a member of the Japanese Society of Radiological Technology, Japan Osteoporosis Society, the Japanese Society of Nutrition and Dietetics, the Japan Geriatrics Society, and Japan Society of Clinical Chemistry.

Atsushi Takigawa received his BS degree from Kyoto University, Japan, in 1974, and received his PhD degree from Kyoto Institute of Technology, Japan, in 1995. Since April 2000, he has been a professor at the Department of Radiological Sciences, Hiroshima Prefectural College of Health Sciences, Hiroshima, Japan. His research interests include radiological technology. He is a member of the Japanese Society of Radiological Technology, Japanese Society of Medical Imaging and Information Sciences, Japan Society of Medical Physics, and Society of Photographic Science and Technology of Japan.

Takeshi Hara received his BS degree in 1994, MS degree in 1995, and PhD degree in 2000 from Gifu University, Japan. Since 2002, he has been an associate professor at the Department of Intelligent Image Information, Division of Regeneration and Advanced Medical Science, Graduate School of Medicine, Gifu University, Japan. His research interests include computer-aided diagnosis system, image analysis and processing, and image evaluation in medicine. He is a member of the Institute of Electronics, Information and Communication Engineers, Japanese Society of Medical Imaging and Information Sciences, Japanese Society of Radiological Technology, and Japanese Society of Medical Imaging Technology.

Xiangrong Zhou received his BS degree from Harbin Institute of Technology, People's Republic of China in 1989, and received his PhD degree from Nagoya University, Japan, in 2000. Since 2002, he has been a research associate at the Department of Intelligent Image Information, Division of Regeneration and Advanced Medical Science, Graduate School of Medicine, Gifu University, Japan. His research interests include computer-aided diagnosis system, medical image analysis and processing, and image evaluation in medicine. He is a member of the Institute of Electronics, Information and Communication Engineers.